2015년 8월

석사학위 논문

Fabrication and optical characterization of Bragg-resonating luminescence semiconductor chip

조 선 대 학 교 대 학 원

화 학 과

박 미 애

Fabrication and optical characterization of Bragg-resonating luminescence semiconductor chip

브래그 공명 발광 반도체 칩의 제조 및 광학적 특성 분석

2015년 8월 25일

조 선 대 학 교 대 학 원

화 학 과

박 미 애

브래그 공명 발광 반도체 칩의 제조 및 광학적 특성 분석

지도교수 손 홍 래

이 논문을 이학석사학위신청 논문으로 제출함.

2015년 5월

조 선 대 학 교 대 학 원

화 학 과

박 미 애

박미애의 석사학위논문을 인준함

위원장 조선대학교 교수 고 문 주 (인)

위 원 조선대학교 교수 이 범 규 (인)

위 원 조선대학교 교수 손 홍 래 (인)

2015년 5월

조 선 대 학 교 대 학 원

TABLE OF CONTENTS

Chapter 2.

Fabrication and optical characterization of Bragg resonance luminescence porous silicon

LIST OF SYMBOLS AND ABBREVIATIONS

PS	Porous Silicon
PBR PS	Photoluminesent Bragg-Reflective Porous Silicon
BRL PS	Bragg Resonance Luminesence Porous Silicon
HF	Hydrofluoric Acid
μm	Micrometer
FE-SEM	Field Emission-Scanning Electron Microscope
FWHM	Full Width at Half Maximum
CCD	Charge-Coupled Detector
a.u.	Arbitrary Units
PL	Photoluminescence
LED	Light Emitting Diode
n	Refractive Index
L	Thickness
nm	Nanometer
FT-IR	Fourier Transform Infrared Spectroscopy
UV-Vis	Ultraviolet-Visible
λmax	Maximum Wavelength
H_2SO_4	Sulfuric acid
H_2O_2	Hydrogen peroxide

LIST OF FIGURES

Figure 9 Reflectivity and PL spectra of monolayer PS and BRL PS: quenching PL spectra of monolayer PS (A), reflectivity spectra of BRL PS (B), and quenching PL spectra of BRL PS (C) under a flux of acetone vapor, respectively. BRL PS etched at 300 mA/cm^2 for 1.5 s and 30 mA/cm^2 for 4.5 s with 55 repeats showed a reflectivity at 629 nm (FWHM 33 nm) and PL at 665 nm (FWHM 27 nm). The different peak wavelength in reflectivity and PL spectra might have resulted from the different incidence angle.

초록

브래그 공명 발광 반도체 칩의 제조 및 광학적 특성 분석

박 미 애
지도교수 : 손 홍 래
자연과학대학 화학과
조선대학교 대학원

Chapter 1. 최근 수 십 년간 전기·전자 및 금속·반도체기술이 눈부신 발전을 이룩하였다면 21세기 현대과학에서는 새로운 형태나 특성을 연구하는 영역으로 나노과학(nanoscience) 및 나노기술(nanotechnology)이 급속히 발전하고 있다. 현대 화학이 여러 분야로 세분화되고, 전문화되어지면서 광화학 (photochemistry)이나 나노화학 (nanochemistry)에 대한 관심도가 매우 높아지고 있다. 특히, 나노(nano) 소재를 이용한 분야가 매우 빠른 속도로 발전하고 있다. 나노과학은 나노소재의 합성 및 응용분야로 분류된다. “나노센서(nanosensor)”는 나노과학의 한 응용분야로서 분자 수준의 조작이 가능한 분자센서(molecular sensor)의 집적화 또는 나노소재 (nanomaterial)나 나노구조물 (nanostructure)의 특성을 이용한 센서를 의미한다. 나노소재로는 나노다공질재료 (nanoporous material), 금속 및 반도체소재의 나노와이어 (nanowire), 나노입자 (nanoparticle), 나노튜브(nanotube) 등이 있으며 기질을 인지(recognition) 또는 감지(sensing)할 수 있는 나노소재로부터 장치(device)를 만들었을 경우 나노센서라 일컫는다.

최근 나노센서 또는 나노바이오센서 등에 대한 관심이 나노과학의 한 분야로서 지대한 관심의 대상이 되고 있는데 그 이유는 고감도, 초소형의 센서 구현을 통해서 생명현상인 분자 간의 상호작용을 나노크기의 수준에서 탐구하려는 학문적인 관심과 함께 응용적인 측면에서 보건의료, 식품, 환경, 국방 등의 다양한 분야에서 활용되는 센서를 개발하기 위한 실질적인 중요성 때문에 학계와 연구소, 그리고 산업체에서 활발히 연구되고 있다. 특히 나노 신소재 개발 분야는 기초과학에서부터 첨단과학까지의 융합학제 (interdisciplinary)간 학문 분야로 미래기술의 선점 및 국가경쟁력 확보에 있어서 우위를 차지하는데 중요한 역할을 할 것으

로 기대된다.

따라서 본 연구논문의 주제는 나노화학 및 유기용매센서 개발의 일환으로 반도체 실리콘 재료를 이용하여 화학센서재료의 개발을 목표로 한다. 연구논문의 구성은 전반부에는 실리콘 웨이퍼를 전기화학적 식각을 통하여 얻어진 가시광선 영역의 광 발광 Bragg 반사체를 가진 다공성 실리콘을 개발하였고, 후반부에는 Bragg 공명 발광을 가진 다공성 실리콘의 제작하고 유기용매를 탐지 하는 센서의 재료로 사용 하였다.

논문의 chapter I 에서 나노센서로 이용된 다공성 실리콘은 실리콘 나노구조물이며, 나노크기의 기공들이 존재하는 간섭 막들의 굴절률의 변화로부터 얻어지는 독특한 광학적 특성인 광 반사(optical reflection)성을 갖는다. 다공성 실리콘은 1950대에 Uhlir에 의해 실리콘 단결정을 전자연마 (electropolishing) 하다가 발견되었으며, 1990년대 다공성 실리콘의 효율적인 발광(luminescence)을 발견한 이래로, 이 분야는 화학 · 물리학적 광학 특성의 연구에 매우 광범위하게 이용되어지고 있다. 다공성 실리콘은 간섭 막의 굴절률 조절로 인해 가시광선 및 적외선 영역에서 특정한 파장에서 보강간섭을 갖는 반사 띠를 갖기 때문에 센서 등 여러 분야에 적용될 수 있는 좋은 소재이다.

Chapter 2. 다공성 실리콘은 간섭 막의 굴절률 조절로 인해 가시광선 및 적외선 영역에서 특정한 파장에서 보강간섭을 갖는 반사 띠를 갖기 때문에 센서 등 여러 분야에 적용될 수 있는 좋은 소재이다. 또한, 바이오센서분야로 이용될 경우 분자인식현상 (molecular recognition event)으로 매 추가 분자를 인식할 때마다 신호를 적립할 수 있는 장점이 있어 인식체가 분자수준의 신호증폭(molecular-level amplification)을 하게 된다. 따라서 선택성을 높이고 탐지한계를 낮추는 방법론을 개선하기위해 다양한 전기화학적 식각방법을 개발한다면 다른 나노소재보다 비교우의에 있을 것으로 사료된다. 본 연구논문의 결과로 Bragg 공명 발광을 가진 다공성 실리콘의 제작으로 Acetone의 229.53 mmHg 가스농도를 감지에 성공하였고, 반사 스펙트럼과 공명이 일어나지 않은 발광스펙트럼보다 훨씬 빠른 시간 내에 탐지하는 걸 알 수 있었다. 본 연구는 다양한 학문 분야의 지식을 바탕으로 아직까지 정확히 확립되지 않은 나노센서, 나노소재의 분석 및 그 응용과 관련된 중요한 정보를 구축하는데 크게 기여할 것으로 사료된다.

Chapter 1.

Fabrication and optical characterization of visible photoluminescent Bragg-reflective porous silicon

1.1. Introduction

Since the discovery of visible photo- and electroluminescence from porous silicon (PS) [1], PS has been intensively investigated for a variety of applications such as chemical [2] and biological sensors [3], medical diagnostics [4], micro chemical reactors [5], and drug delivery [6]. PS is an ideal candidate for gas- or liquid-sensing applications, since it has a very large specific surface area in the order of few hundreds m^2/cm^3. The direction of pores and pore diameters depend on surface orientations, doping level and type, the temperature, the current density, and the composition of the etching solution [7]. The main techniques investigated to achieve the signal transduction are capacitance [8], resistance [9], photoluminescence (PL) [10], and reflectivity [3].

Typically, PS prepared from p-type silicon wafer under dark condition exhibits well defined Fabry-Pérot fringes in the optical reflectivity spectrum. However, PS prepared from n-type silicon wafer under white light shows a strong naked-eyed photoluminescence under Ultraviolet (UV) light irradiation. Capillary condensation of analytes in the pores leads to a shift in the Fabry-Pérot fringes by the modification of the refractive index of PS and an electron transfer from analyte to silicon quantum dot (Si QD) in PS causes a quenching photoluminescence of quantum-confined Si QD. Recently, PS samples exhibiting both strong photoluminescence and well defined

Fabry-Pérot fringes were reported. Both photoluminescence and reflectivity of PS were used to detect organic vapors [11] and nerve agent simulants [12].

PS is an excellent material to produce photonic crystals which are periodic arrays of dielectric materials having photonic band gaps similar to the electronic bands of solid crystals. Both, the structure and the refractive index contrast between the dielectric materials play a crucial role on the photonic properties. Berger et al. proved the feasibility of fabrication of high reflectivity porous silicon mirrors, Bragg reflectors and Rugate filters [13]. The Bragg reflector is characterized by its central wavelength λ_0, and by the reflection bandwidth which is determined mainly by the index contrast. In some cases, narrow reflection bandwidth might be useful for sensing applications. A strong red PL is observed from PS prepared from an electrochemical etching of lightly doped n-type Si wafer, however Bragg reflection is usually observed from PS prepared by an electrochemical etching of highly doped p-type Si wafer. To date, there is no report on the formation of photoluminescent Bragg-reflective porous silicon (PBR PS) showing a strong naked-eyed photoluminescence as well as a strong optical reflectivity in the visible range from the same sample. Here, we reported the synthesis and characterization of PBR PS exhibiting both optical reflectivity and strong photoluminescence prepared from highly doped n-type silicon wafers through the electrochemical etching.

1.2 Experiment

1.2.1 Preparation of PBR PS

PBR PS samples were obtained by an electrochemical etching of the phosphors-doped n-type Si <100> substrate (Prime grade, Siltronix Inc, Archamps, France) with a resistivity in the range of 0.001 ~ 0.003 Ω•cm. The galvanostatic etch was carried out in Teflon cell by using a two-electrode configuration with a Pt ring counter electrode. The anodization current was supplied by a Keithley 2420 high-precision constant current source (Keithley Instruments Inc, Cleveland, OH, USA). Galvanostatic etching was performed under the illumination with a 300 W tungsten filament bulb for the duration of etch. PBR PS showing the reflectivity of 748 nm was prepared by applying 270 mA/cm^2 for 1.2 s as high current and 70 mA/cm^2 for 5.2 s as low current with 80 repeats. The etching solution consists of 3:1 by volume mixture of absolute ethanol (ACS reagent, Merck KGaA, Darmstadt, Germany) and aqueous 48% Hydrofluoric Acid (HF) (ACS Reagent, J.T. Baker, PA, USA). PBR PS showing the reflectivity of 615 nm was prepared by applying 270 mA/cm^2 for 1.2 s as high current and 70 mA/cm^2 for 4.2 s as low current with 80 repeats. The etching solution consists of 1:1 by volume mixture of absolute ethanol and aqueous 48% HF. Electropolishing condition is 270 mA/cm^2 for 60 s to obtain a free-standing PBR PS. All samples were then rinsed several times with ethanol and dried under argon atmosphere prior to use.

1.2.2 PL and reflectance measurements

Steady-state PL spectra were obtained with an Ocean Optics S2000 spectrometer (Ocean Optics, Inc, Dunedin, FL, USA) fitted with a fiber optic probe. The excitation source was a UV Light Emitting Diode (LED) (λ_{max}=400 nm) focused on the sample (at 45^0 angle to the normal of the surface) by means of a separate fiber. The light was collected at 90^0 angle to the incident light source with a fiber optic. Spectra were recorded with a harge-Coupled Detector (CCD) in the wavelength range of 400 to 900 nm. Interferometric reflectance spectra of PS samples were recorded by using an Ocean Optics S2000 spectrometer. A tungsten light source was focused onto the center of a PS surface. Spectra were recorded with a CCD detector in the wavelength rang 400 ~ 1200 nm. The illumination of the surface as well as the detection of the reflected light were performed along an axis coincident with the surface normal. Morphologies of PS were obtained by a cold field emission scanning electron microscopy (FE-SEM, S-4800, Hitachi, Ltd., Chiyoda, Tokyo, Japan).

1.3 Results and Discussion

There has been growing interest in the development of efficient control for the preparation of PS multilayer stacks. As porous silicon porosity is a function of the current density, different refractive indexes of porous silicon layers can be built up, one after another, on a silicon substrate in the vertical direction by alternating the applied current densities during the electrochemical etching. Bragg reflector is a structure which consists of an alternating sequence of layers made of two different refractive indices. Bragg reflector exhibits a high reflectivity band with a Bragg wavelength, λ_o, depending on the thickness of the layers (L_1, L_2) and the corresponding refractive indices (n_1, n_2). The m^{th} order of the Bragg peak is given by:

$$m\lambda_0 = 2(L_1 n_1 + L_2 n_2) \quad (1)$$

The quality of Bragg reflector PS in photonics can be improved when the refractive index contrast between layers is increased. The band gap widening of PS due to quantum confinement effects leads to a decrease of the extinction coefficient k, making porous silicon transparent in the infrared region. PS has a low extinction coefficient in near Infrared Spectroscopy (IR) range (1000-2500 nm) but a strong extinction coefficient in Ultraviolet-Visible (UV-Vis) range (300-1000 nm). PS Bragg reflector with a reflection bandwidth of 300 nm in the IR range has been demonstrated with good spectral behavior due to the low absorption of PS [14].
The reflectivity of Bragg reflector is determined by the number of layer

pairs and the refractive index contrast Δn between the layers. Bragg reflector is characterized by its central wavelength λ_o (at normal incidence) and by the reflection bandwidth $\Delta\lambda$ which is determined mainly by the index contrast. These two parameters are defined, respectively, by the relationships (1) and (2) [14].

$$\triangle\lambda = \frac{2\lambda_0 \triangle n}{\pi n} \tag{2}$$

with

$$\triangle n = n_1 - n_2$$

$$n = \frac{n_1 - n_2}{2}$$

Recently, there are several reports for the generation of Bragg reflector PS to achieve the same degree of performance in the visible range, even though PS has a strong absorption coefficient from the visible to UV region [15]. For sensing application, the Bragg reflector PS with narrow reflection bandwidth obtained by tuning the refractive index and etching time is desirable. The Bragg reflector PS was used for the detection of organic vapors [16, 17] and toxic gases [18], and drug delivery materials [19, 20]. Moreover, to specify an analyte with a sensor, multi-transduction modes within the PS would be useful. The Bragg reflector PS exhibiting both strong PL and Fabry-Pérot fringes was reported [11, 12]. Here, we report the synthesis and characterization of PBR PS exhibiting both optical reflectivity and strong PL prepared from highly doped n-type silicon wafers through the electrochemical etching.

PBR PS exhibiting both Bragg reflection and strong PL in the visible range

was successfully fabricated. PBR PS showing the reflectivity at 748 nm was prepared by applying the current of 270 mA/cm^2 for 1.2 s and 70 mA/cm^2 for 5.2 s with 80 repeats in etching solution of 3:1 volume mixture of absolute ethanol and aqueous 48% HF. The reflectivity and PL spectra and photographs of PBR PS were shown in Figure 1. As-prepared PBR PS exhibits strong reflection at 748 nm under white light and strong red PL at 688 nm under black light.

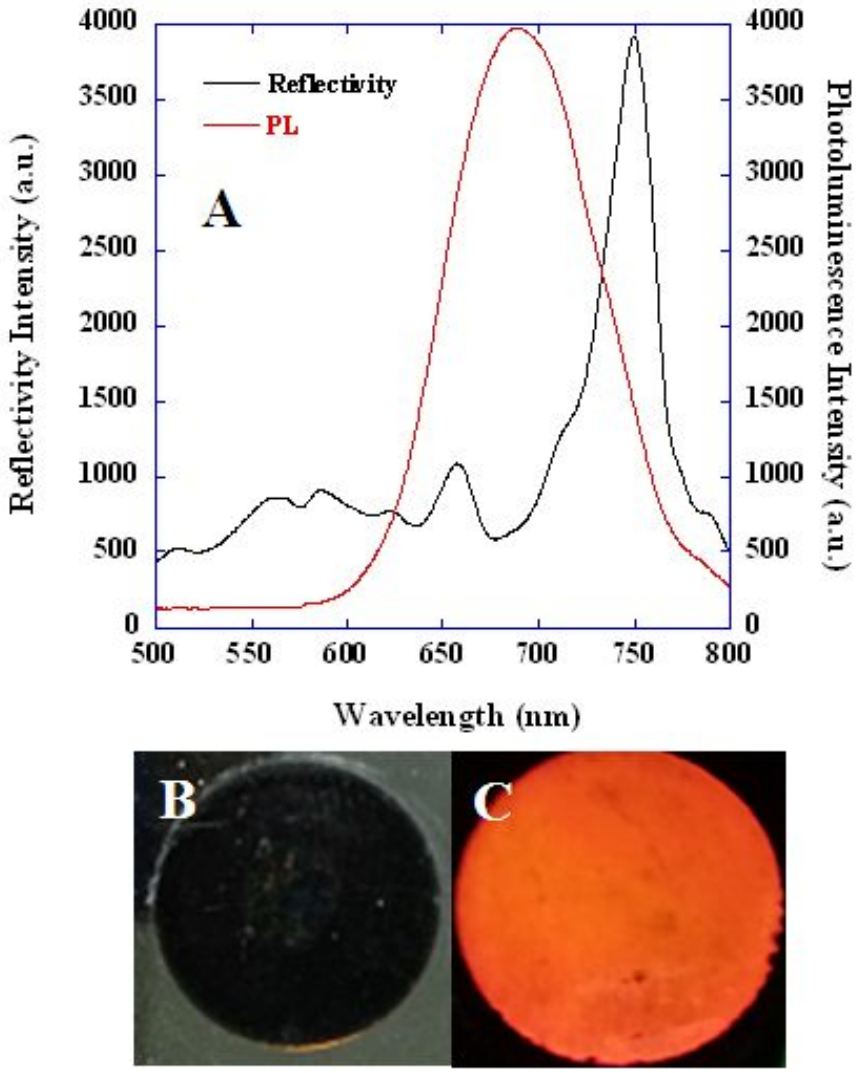

Figure 1. Reflectivity and PL spectra of PBR PS prepared at the current of 270 mA/cm^2 for 1.2 s and 70 mA/cm^2 for 5.2 s with 80 repeats in etching solution of 3:1 volume mixture of absolute ethanol and aqueous 48% HF (A) and photographs under white light (B) and black light (C).

Another PBR PS showing the reflectivity at 615 nm was prepared by changing the low current etching time to 4.2 s and the etching solution of 1:1 volume mixture of absolute ethanol and aqueous 48% HF. As shown in Figure 2, as-prepared PBR PS exhibits strong red color reflection at 615 nm under white light as well as strong red PL at 642 nm under black light. The relationship between the reflection wavelengths and the repeat number was shown in Figure 3A. As the repeat number increases, the reflection wavelength shifts to the shorter wavelength without changing of full width at half maximum (FWHM). Such a blue shift is characteristic of an increase in the etching depth of the multilayers. Figure 3B shows PL spectra according to the repeat number. For the repeat number of 70 and 80, PBR PS shows typical broad PL spectra at 650 nm. However, in the cases of 60 and 70 repeat, PL spectra show a Bragg-reflective PL behavior at the center of PL wavelength. Currently, the Bragg-reflective PL property of PBR PS is under investigation.

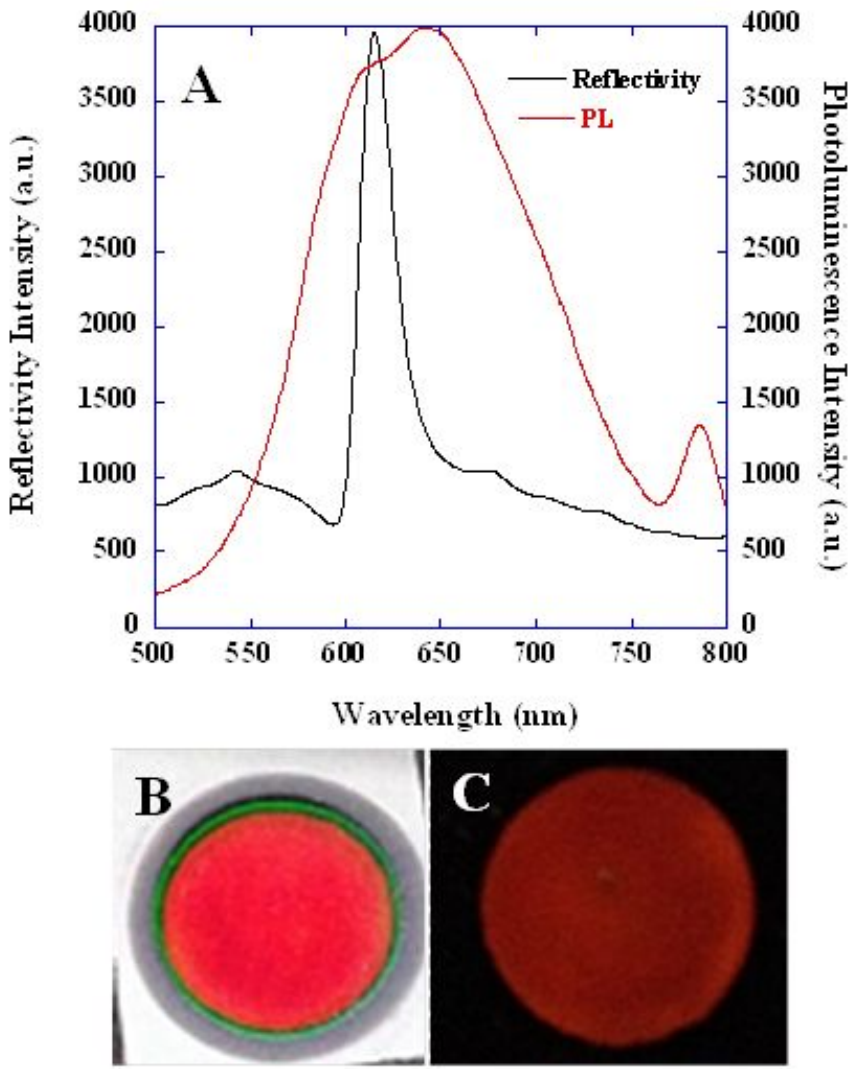

Figure 2. Reflectivity and PL spectra of PBR PS prepared at the current of 270 mA/cm^2 for 1.2 s and 70 mA/cm^2 for 4.2 s with 80 repeats in etching solution of 1:1 volume mixture of absolute ethanol and aqueous 48% HF (A) and photographs under white light (B) and black light (C).

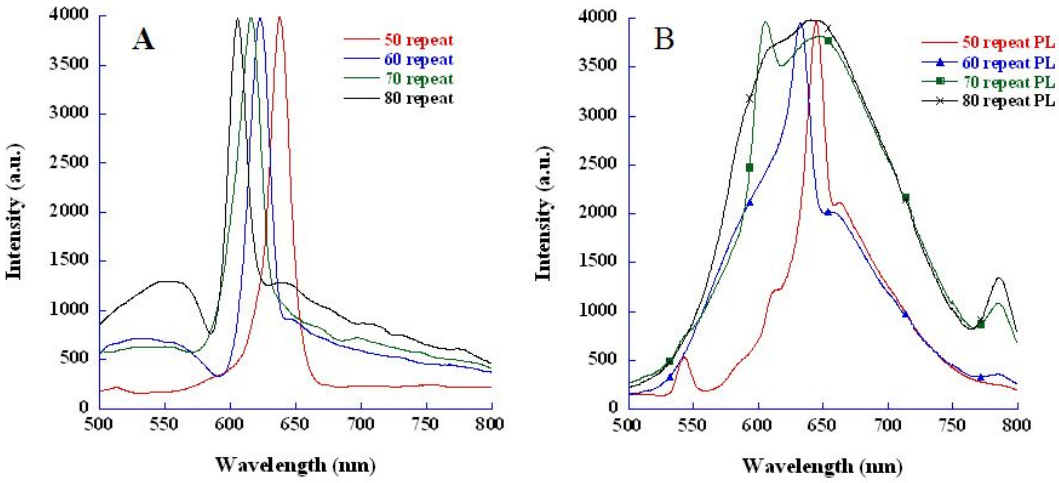

Figure 3. Reflectivity of PBR PS prepared at the current of 270 mA/cm^2 for 1.2 s and 70 mA/cm^2 for 4.2 s according to repeat number from 50 to 80 showing the blue shift as the repeat number increases.

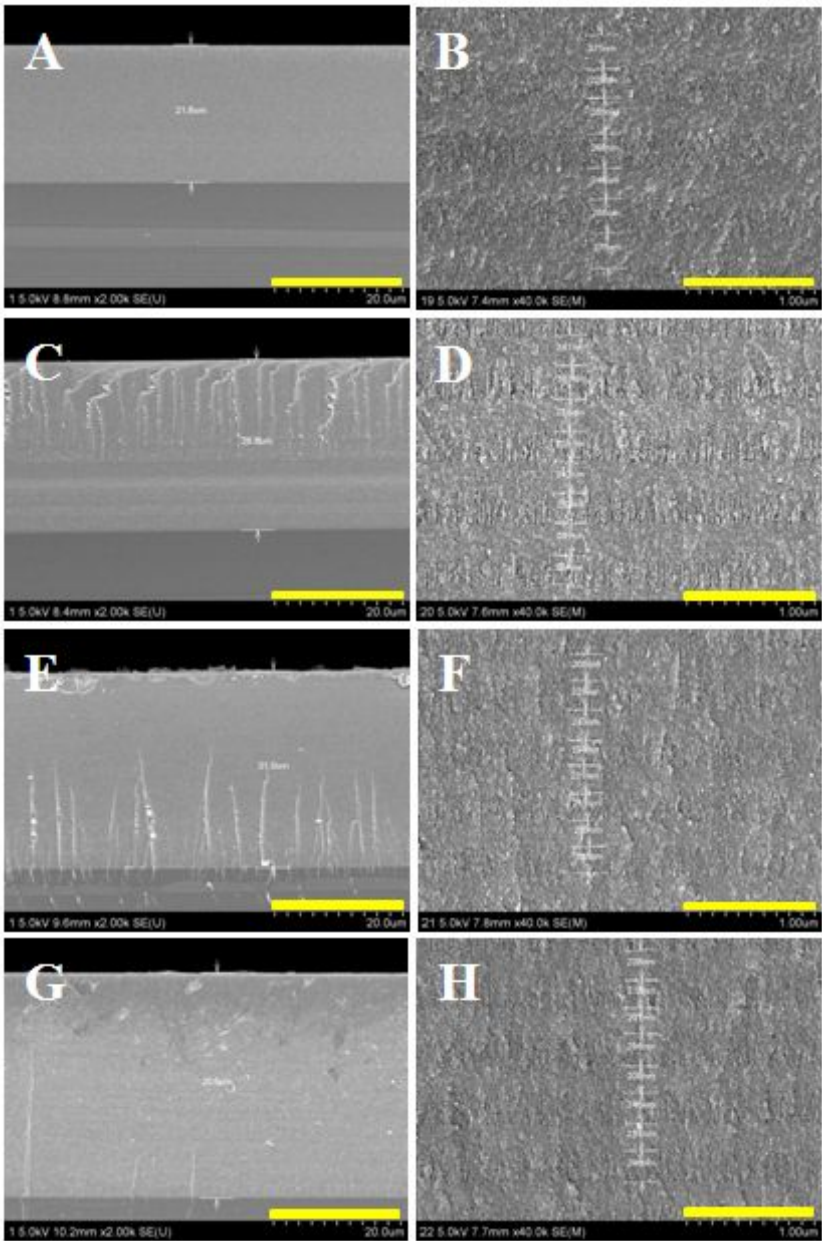

Figure 4. Cross-section FE-SEM images of PBR PS prepared at the current of 270 mA/cm^2 for 1.2 s and 70 mA/cm^2 for 4.2 s with the repeat number of 50

(A), 60 (C), 70 (E), 80 (G) and their enlarged images with the repeat number of 50 (B), 60 (D), 70 (F), 80 (H), respectively. Scale bars for (A), (C), (E), and (G) are 20 μm and for (B), (D), (F), and (H) are 1 μm, respectively.

Etching depths of PBR PS according to repeat number from 50 to 80 were obtained using cold FE-SEM and shown in Figure 4. The etching depths of PBR PS with 50, 60, 70, and 80 repeats were 21, 26, 31, and 36 micrometers, respectively. The etching depth showed a linear profile with the increase of repeat number. From the enlarged images, all depths of layers for high and low porosity were about 200 nm. A repeating etching process results in two small different refractive indices causing the narrow reflection bandwidth of PBR PS.

To investigate the optical properties of PBR PS in detail, as-prepared PBR PS lift off from the silicon substrate. After the generation of PBR PS, the resulting PBR PS films were removed from the silicon substrate by applying an electropolishing current of 270 mA/cm^2 for 60 s to obtain a free-standing PBR PS film. Figure 5 shows reflectivity and PL spectra of free-standing PBR PS film in both front (A and C) and back side surface (B and D). Insets are photographs free-standing PBR PS under white light (A and C) and black light (B and D). The front side surface of PBR PS shows both reflectivity and PL, however the back side surface of free-standing PBR PS shows only reflectivity without PL. Reflectivity on front and back side surface of free-standing PBR PS occurs at the same wavelength.

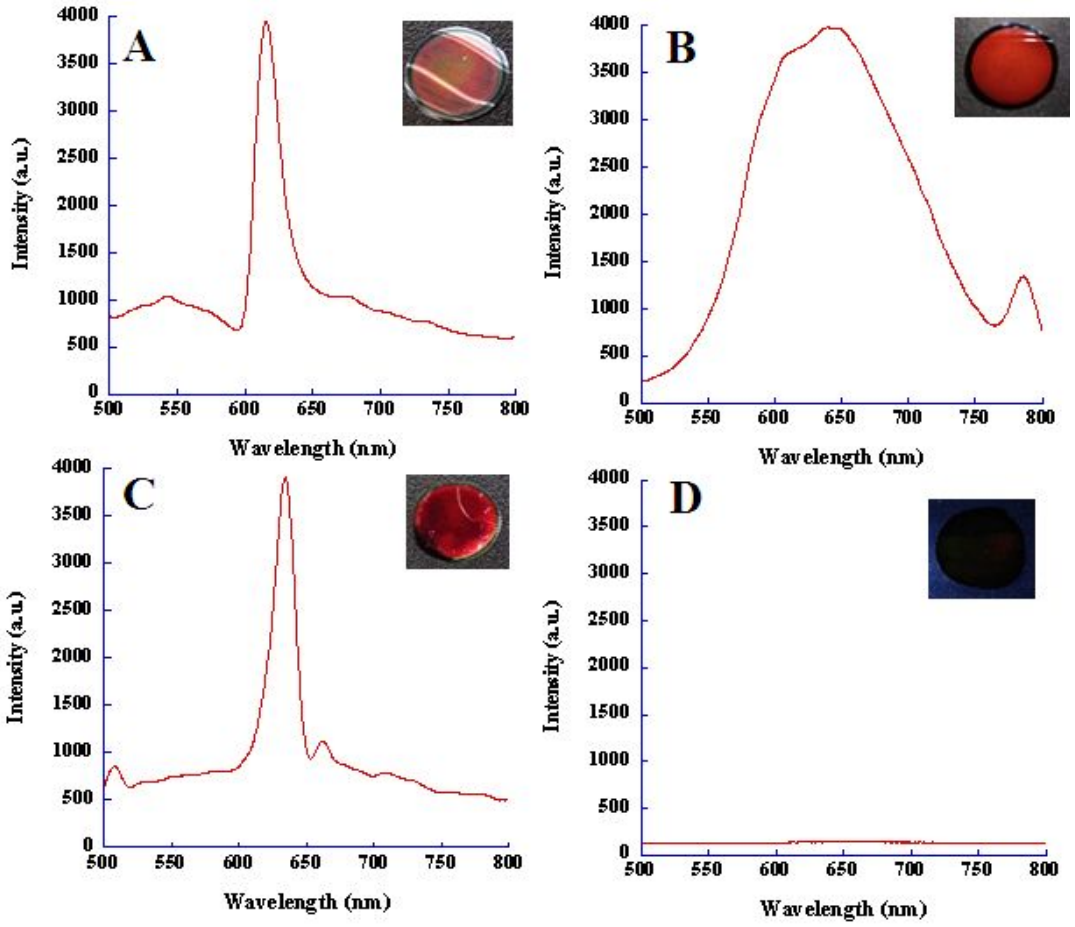

Figure 5. Reflectivity and PL spectra of free-standing PBR PS film prepared at the current of 270 mA/cm^2 for 1.2 s and 70 mA/cm^2 for 4.2 s with 80 repeat in both front (A and C) and back side surface (B and D). Insets are photographs free-standing PBR PS under white light (A and C) and black light (B and D).

Figure 6 shows FE-SEM images of front (A) and back (C) side surface of free-standing PBR PS and cross-section image of free-standing PBR PS (B).

Figure 6A shows that the pore size of free-standing PBR PS is in the range of 2 to 5 nm and Figure 6B shows two different porosity layers. Figure 6C shows a huge pore structure at the back side surface of free-standing PBR PS. This result might be caused during the electropolishing process and may place only top portion of back side surface of free-standing PBR PS.

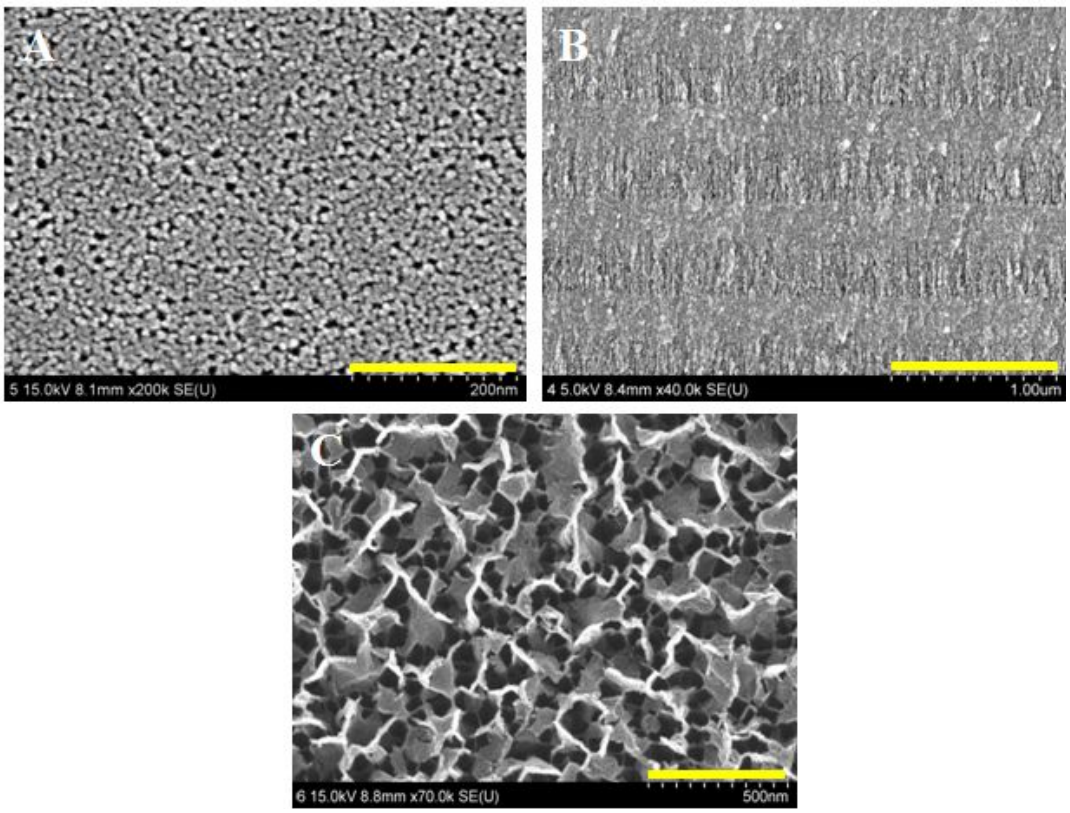

Figure 6. FE-SEM images of front (A) and back (C) side surface of free-standing PBR PS and cross-section image of free-standing PBR PS (B). Scale bars for (A), (B), and (C) are 200 nm, 1 μm, 500 nm, respectively.

1.4. Conclusion

The synthesis and characterization of PBR PS exhibiting both optical reflectivity and strong photoluminescence from highly doped n-type silicon wafers through the electrochemical etching were reported. Two successive PBR PS samples were fabricated. PBR PS exhibits strong red color reflection at 615 nm under white light as well as strong red PL at 642 nm under black light. As the repeat number increases, the reflection wavelength shifts to the shorter wavelength. For the repeat number of 70 and 80, PBR PS shows typical broad PL spectra at 650 nm. However, in the case of 60 and 70 repeat, PL spectra show a Bragg-reflective PL behavior at the center of PL wavelength. The etching depth showed a linear profile with the increase of repeat number. The optical properties of free-standing PBR PS film were investigated. The front side surface of PBR PS shows both reflectivity and PL, however the back side surface of free-standing PBR PS shows only reflectivity without PL.

1.5. References

[1] L. T. Canham. *Appl. Phys. Lett.* 57(10), 1046 **(1990).**

[2] H. Sohn, S. Letant, M. J. Sailor, and W. C. Trogler, *J. Am. Chem. Soc.* 122, 5399 **(2000).**

[3] V. S. Lin, K. Motesharei, K. S. Dancil, M. J. Sailor, and M. R. Ghadiri, *Science* 278, 840 **(1997).**

[4] J.H. Park, L. Gu, G.Von Maltzahn, E. Ruoslahti, S. N. Bhatia, M. J.Sailor, *Nat. Mater.* 8, 331 **(2009).**

[5] T. Laurell, J. Drott, L. Rosengren, K. Lindström, *Sensor. Actuat B-Chemical.* 31, 161 **(1999).**

[6] E. J. Anglin, L. Cheng, W. R. Freeman, M. J. Sailor, *Adv. Drug Deliver. Rev.* 60, 1266 **(2008).**

[7] R. L. Smith, S. D. Collins, *J. Appl. Phys.* 71, R1 **(1992).**

[8] R. C. Erson, R. S. Muller, C. W. Tobias, *Sensor. Actuat. A-Phys.* 23, 835 **(1990).**

[9] M. Ben-Chorin, A. Kux, and I. Schechter, *Appl. Phys. Lett.* 64, 481 **(1994).**

[10] J. M. Lauerhaas and M. J. Sailor, *Science* 261, 1567 **(1993).**

[11] S. G. Lee, Y. Koh, S. Jang, J. Kim, H. G. Woo, S. Kim, H. Sohn, *J. Nanosci. Nanotechnol.* 10, 3266 **(2010).**

[12] S. Kim, B. Cho, and H. Sohn, *Nanoscale Res. Lett.* 7, 527 **(2012).**

[13] M. G. Berger, R. Arens-Fisher, M. Thönissen, M. Krüger, S. Billat, H. Lüth, S. Hilbrich, W. Theiss, P. Grosse, *Thin. Solid. Films.* 297, 237 **(1997).**

[14] J. Charrier, P. Pirasteh, Y. G. Boucher, M. Gadonna, *Micro. Nano. Lett.* 7, 105 **(2012).**

[15] R. Naval, M. B. De La Mora, J. Tagüeña-Martínez, J. A. Del Río, *Phys.*

Status. Solidi. C. 6, 1721 **(2009).**

[16] P. A. Snow, E. K. Squire, P. St J Russell, L. T. Canham, *J. Appl. Phys.* 86, 1781 **(1999).**

[17] S. G. Kim, S. Kim, Y. C. Ko, S. Cho, H. Sohn, *Colloids. Surf A-Physicochem. Eng. Aspects.* 313, 398 **(2008).**

[18] S. Jang, Y. Koh, J. Kim, J. Park, C. Park, S. J. Kim, S. Cho, Y. C. Ko, H. Sohn, *Mater. Lett.* 62, 552 **(2008).**

[19] Y. Koh, S. Jang, J. Kim, S. Kim, Y. C. Ko, S. Cho, H. Sohn, *Colloids. Surf. A-Physicochem. Eng. Aspects.* 313, 328 **(2008).**

[20] C. Park, J. Kim, S. Jang, H. G. Woo, Y. C. Ko, H. Sohn, *J. Nanosc.i Nanotechnol.* 10, 3375 **(2010).**

Chapter 2.

Fabrication and optical characterization of Bragg resonance luminescence porous silicon

2.1 Introduction

Since the discovery of photoluminescent porous silicon (PS) [1]. it has been attracted for a variety of applications such as chemical and biological sensors and drug delivery system [2-5]. The main sensing techniques investigated to achieve signal transduction are capacitance [6], resistance [7], photo-luminescence (PL) [8] and reflectivity [9]. Typically, PS exhibiting well defined reflection peak in the optical reflectivity spectrum can be prepared with p-type silicon wafer under dark condition. Sensing molecules such as toxic gases [10-12], solvents [13], DNA [3] and proteins [14,15] can lead to a shift in the reflection peak by modification of the refractive index of PS. However, luminescent PS samples are usually prepared by a galvanostatic photoetch of n-type silicon wafer under illumination condition. As far as we know, this light emission most likely results from quantum confinement effects within silicon nanocrystallites. Photoluminescence intensity of PS depends on the etching conditions [16] as well as the presence of surface adsorbates [17]. Organic vapors have been detected quantitatively by the quenching of PL of the quantum-confined silicon crystallites in PS [18]. The Bragg reflector is characterized by its central wavelength λ_0, and by the reflection bandwidth which is determined mainly by the index contrast. In many cases, narrow reflection bandwidth is highly useful for sensing applications. A strong red PL is observed from PS prepared from an electrochemical etching of lightly doped n-type Si wafer, and Bragg reflection is usually observed from PS prepared by an

electrochemical etching of highly doped p-type Si wafer. To date, there is no report on the formation of enhanced luminescence porous silicon based on Bragg resonance showing both a strong narrow naked-eyed photoluminescence and a strong optical reflectivity in the visible range from the same sample. This can be highly useful for sensing applications, since the signal changes can be measured simultaneously by two different sensing mechanisms, the quenching of PL and shift of the reflectivity, which can give a huge advantage when comes to selectivity. Here, we reported the synthesis and characterization of Bragg resonance luminescence porous silicon (BRL PS) exhibiting both optical reflectivity and strong narrow visible photoluminescence prepared from highly doped n-type silicon wafers through the electrochemical etching.

2.2 Experiment

2.2.1 Preparation of BRL PS

BRL PS samples were obtained by an electrochemical etching of the phosphors-doped n-type Si <100> substrate (Sino-American Silicon Products Inc.) with a resistivity in the range of 0.001 ~ 0.003 Ω•cm. The galvanostatic etch was carried out in Teflon cell by using a two-electrode configuration with a Pt ring counter electrode. The anodization current was supplied by a Keithley 2420 high-precision constant current source (Keithley Instruments Inc., Cleveland, OH, USA). Galvanostatic etching was performed under the illumination with a 300 W tungsten filament bulb for the duration of etch. The commercial Si wafer were cut 1.5 x 1.5 cm^2 squares and washed

with water and acetone and them were immersed in oxidant solution containing H_2SO_4 (97 %) and H_2O_2 (35 %) in a volume ratio 3:1 for 10 min under room temperature to entirely remove organics and to form a thin oxide layer. Then they were etched with 5 % HF aqueous solution for 3 min under room temperature and the fresh Si surfaces were H-terminated. BRL PS showing the reflectivity of 615 nm was prepared by applying 30 mA/cm^2 for 4.5 s as low current and 300 mA/cm^2 for 1.5 s as high current with 50, 55, and 60 repeats. The etching solution consists of 1:1 by volume mixture of absolute ethanol (ACS reagent, Merck KGaA, Darmstadt, Germany) and aqueous 48% HF (ACS Reagent, J.T. Baker, PA, USA). For comparison, typical monolayer photoluminescence PS samples were obtained by an electrochemical etching of the n-type Si <100> substrate (phosphors-doped, resistivity of 1-10 Ω•cm) and prepared by applying 200 mA/cm^2 for 300 s. The etching solution consists of a 1:1 by volume mixture of absolute ethanol and aqueous 48% HF. All samples were then rinsed several times with ethanol and dried under argon atmosphere prior to use. The samples were then mounted in a glass chamber connected to a Schlenk line. The Schlenk line was connected to a direct-drive vacuum pump. The chamber was pumped to < 1 m Torr between gas exposures.

2.2.2 PL and reflectance measurements

Steady-state PL spectra were obtained with an Ocean Optics S2000 spectrometer (Ocean Optics, Inc., Dunedin, FL, USA) fitted with a fiber optic probe. The excitation source was a UV LED (λ_{max} = 400 nm) focused on the sample (at 450 angle to the normal of the surface) by means of a separate fiber. The light was collected at 90^0 angle to the incident light source with a fiber optic. Spectra were recorded with a CCD-detector in the wavelength range of 400 to 900 nm. Values of percent quenching are reported as $(I_0\text{-}I)/I_0$, where I_0 is the initial intensity of the luminescence of BRL, integrated between 400 and 900 nm, in the absence of quencher and I is the integrated luminescence intensity of BRL in the presence of analyte. Interferometric reflectance spectra of PS samples were recorded by using an Ocean Optics S2000 spectrometer. A tungsten light source was focused onto the center of a PS surface. Spectra were recorded with a CCD detector in the wavelength rang 400~1200 nm. The illumination of the surface and the detection of the reflected light were performed along an axis coincident with the surface normal. Morphologies of PS were obtained by a cold field emission scanning electron microscopy (FE-SEM, S-4800, Hitachi, Ltd., Chiyoda, Tokyo, Japan).

2.3 Results and Discussion

The wave properties of light make perfect reflectance possible in stratified dielectric media over all spectral ranges due to interference phenomena. In a single layer of PS, the phase shifts imparted on propagating waves at dielectric interfaces may result in constructive and destructive interference. The optical spectrum from a single layer PS is governed by the

Fabry-Pérot relationship. The wavelength of a peak in the reflectivity spectrum is given by Eq. (1):

$$m\lambda = 2nd \bullet \sin\theta \tag{1}$$

where m is the spectral order of the optical fringe, the wavelength, n the refractive index of the film, and d its thickness.

There has been growing interest in the development of efficient control for the preparation of PS multilayer stacks. As porous silicon porosity is a function of the current density, porous silicon layers having different refractive indexes can be built up, one after another, on a silicon substrate vertically by alternating the applied current densities during the electrochemical etching. Bragg reflector is a structure which consists of an alternating sequence of layers made of two different refractive indices. For repeating layers of alternating thickness and refractive index, many interferences may coherently interact to produce high reflectivity at certain points in the spectrum. When a periodicity is enforced by alternating between two layers of thickness d_i and refractive index n_i such that

$$n_1 d_1 = n_2 d_2 = \lambda/4 \tag{2}$$

peak reflectivity increases rapidly with the number of bilayers N and is given by [19]

$$R \simeq \left(\frac{1-(n_s/n_a)(n_2/n_1)^{2N}}{1+(n_s/n_a)(n_2/n_1)^{2N}}\right)^2 \tag{3}$$

where it is assumed that $n_2 > n_1$ and the substrate refractive index ns is

similar to that of the layers; n_a is the refractive index of the ambient. While this reflectivity is achieved for the design wavelength λ_c, for a sufficient refractive index contrast n_2/n_1 a wide band of perfect reflectivity centered at λ_0 may be observed. The spectral width of the photonic band gap is given by

$$\frac{\triangle\lambda}{\lambda_0} = \frac{4}{\pi} sin^{-1} \frac{n_2 - n_1}{n_2 + n_1} \quad (4)$$

The quality of Bragg reflector PS in photonics can be improved by increasing the refractive index contrast between layers. The bandgap widening of PS due to quantum confinement effects leads to a decrease of the extinction coefficient k, making porous silicon transparent in the infrared region. PS has a low extinction coefficient in near IR range (1000-2500 nm) but a strong extinction coefficient in UV-Vis range (300-1000 nm). PS Bragg reflector with a reflection bandwidth of 300 nm in the IR range has been demonstrated with good spectral behavior due to the low absorption of PS.

Recently, there are several reports for the generation of Bragg reflector PS to achieve the same degree of performance in the visible range, even though PS has a strong absorption coefficient from the visible to UV region. For sensing application, the Bragg reflector PS with narrow reflection bandwidth obtained by tuning the refractive index and etching time is desirable. The Bragg reflector PS is an excellent medium for the detection of organic vapors and toxic gases, and drug delivery material. Moreover, to specify an analyte with a sensor, multi-transduction mode within the same sample of PS gives an extra advantage. Previously, the Bragg reflector PS exhibiting both strong PL and Fabry-Pérot fringes was reported . However, the red strong PL peak of Bragg PS in the report mentioned above was similarly broad to that of monolayer PS.

BRL PS exhibiting both sharp reflection and PL peaks resulted from Bragg resonance in the visible range was successfully fabricated. BRL PS showing

the luminescence at 702 nm with an excitation wavelength of 400 nm was prepared by applying the current of 360 mA/cm^2 for 1.6 s and 75 mA/cm^2 for 3.6 s with 50 repeats in etching solution of 1:1 volume mixture of absolute ethanol and aqueous 48% HF. For comparison, typical monolayer PS showing the luminescence at 655 nm and prepared by applying 200 mA/cm^2 for 300 s. The PL spectra for both monolayer PS and BRL PS were shown in Figure 1. The monolayer PS showed a broad PL spectrum with a full width at half maximum (FWHM) of 125 nm. In contrast, BRL PS exhibited sharp PL peak which reached FWHM of 14 nm, arising from broad PL spectrum. This sharp PL of BRL PS presumably originated from the result of Bragg resonance in PS multilayer.

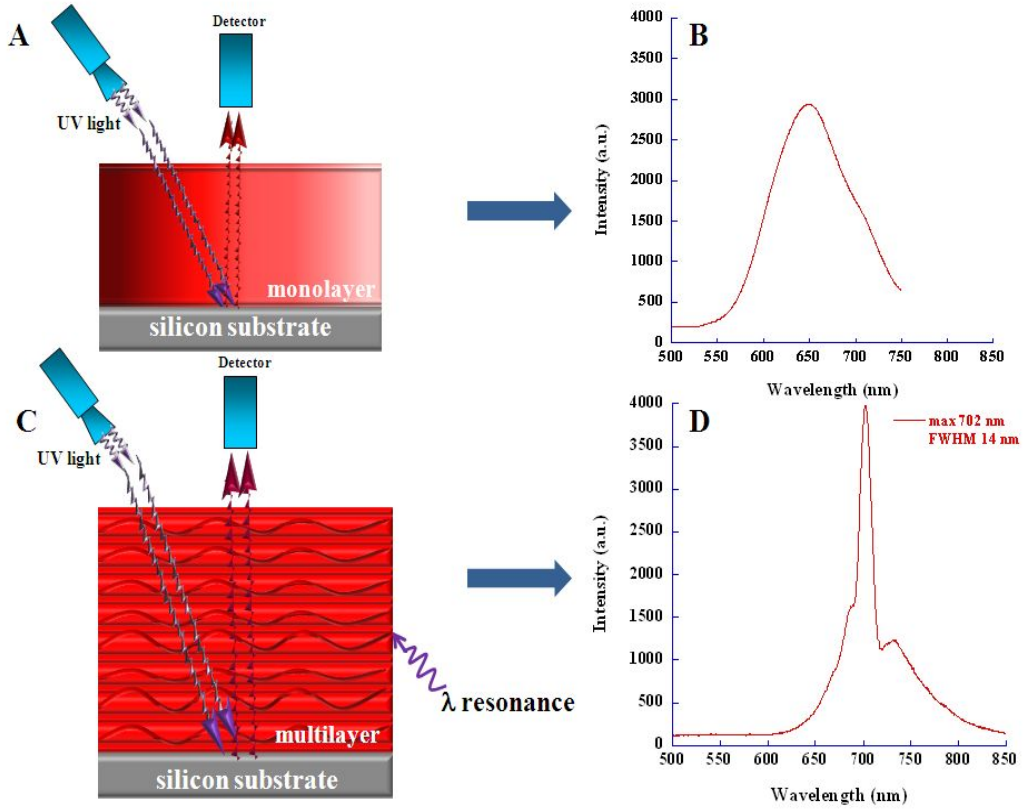

Figure 7. Schematic diagrams and PL spectra for the monolayer PS (A and B) and BRL PS (C and D).

Cross-sectional FE-SEM images of BRL PS with repeat numbers of 50 and 60 were obtained using cold FE-SEM and shown in Figure 2. Both images illustrate that a repeating etching process results in two distinct refractive indices. The each layer depths of BRL PS for both 50 and 60 repeats were about 250 nm. The porosities of high and low refractive layers measured from monolayer PS samples etched at 360 and 75 mA/cm^2 were about 80

and 70 %, respectively. The refractive index range of above PS porosity is from 1.3 to 1.5 according to Bruggeman approximation. The above result suggests that the first-order reflectivity peak of BRL PS is expected to be centered at approximately 1400 nm which indicates that the second-order reflectivity peak should appear at about 700 nm. Therefore, we can reasonably conclude that the sharp PL peak at 700 nm of BRL PS is the second-order luminescence reflectivity peak by Bragg resonance phenomenon.

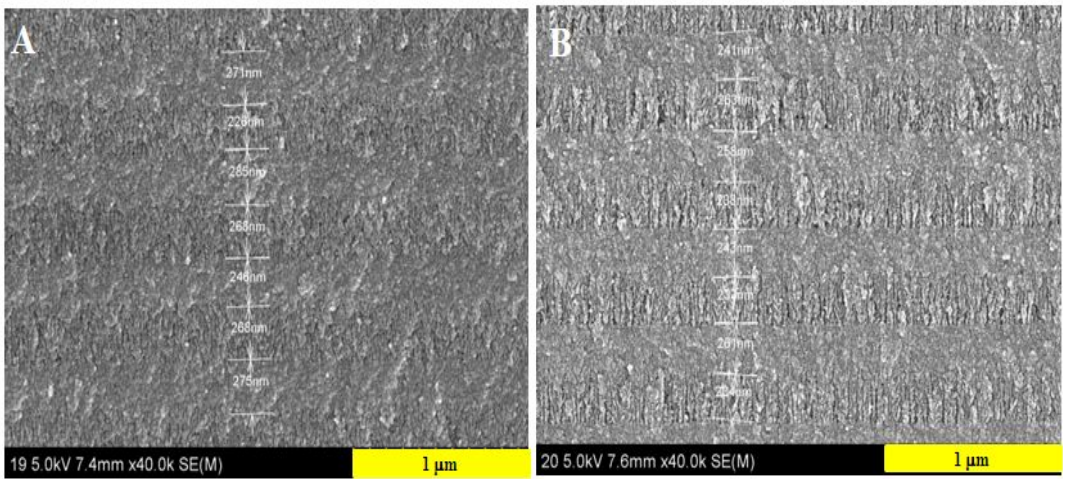

Figure 8. Cross-section FE-SEM images of BRL PS with the repeat number of 50 (A) and 60 (B). Scale bars for A and B are 1 μm.

To investigate the Bragg-reflective PL property, the monolayer PS and BRL PS samples etched at 300 mA/cm^2 for 1.5 s and 30 mA/cm^2 for 4.5 s with 55 repeats, were placed in an exposure chamber fitted with an optical window and then exposed to a vapor flux of acetone (229.53 mmHg at 25 ℃) with a constant argon flow rate of 0.1 L/min. Optical reflectivity and luminescence spectra as shown in Figure 3 were measured simultaneously using a

tungsten-halogen lamp and 400 nm UV LED.

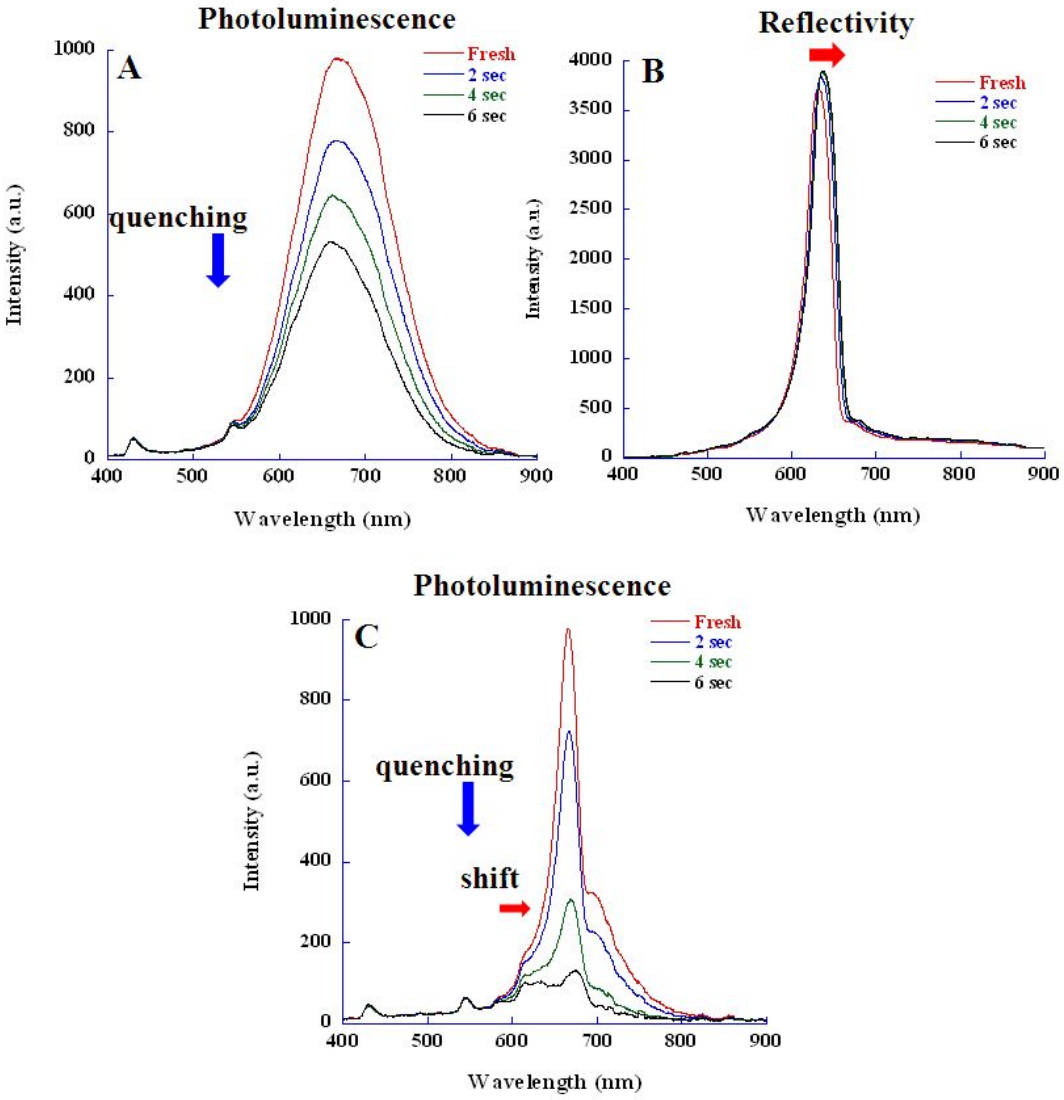

Figure 9. Reflectivity and PL spectra of monolayer PS and BRL PS: quenching PL spectra of monolayer PS (A), reflectivity spectra of BRL PS (B), and

quenching PL spectra of BRL PS (C) under a flux of acetone vapor, respectively. BRL PS etched at 300 mA/cm^2 for 1.5 s and 30 mA/cm^2 for 4.5 s with 55 repeats showed a reflectivity at 629 nm (FWHM 33 nm) and PL at 665 nm (FWHM 27 nm). The different peak wavelength in reflectivity and PL spectra might have resulted from the different incidence angle.

After an exposure of acetone vapor for 6 sec, 48% of luminescence of monolayer PS was quenched without a shift of luminescence wavelength maximum. In the case of BRL PS, the reflection wavelength shifted to longer wavelengths due to an increase in refractive indices of the porous medium, consistent with the replacement of a significant amount of empty pore volume with organic vapors by adsorption. However, 76% of narrow enhanced luminescence based on Bragg resonance in BRL PS quenched dramatically along with 11 nm of red shift. This larger change in quenching PL of BRL PS compare to that of the monolayer PS, is due to the decrease in enhancement effect of luminescence. It should be also noted that the red shift of Bragg resonance luminescence peak is due to the adsorption by organic vapor in pores.

2.4 Conclusion

The synthesis and characterization of BRL PS exhibiting both Bragg reflectivity and Bragg photoluminescence from highly doped n-type silicon wafers through the electrochemical etching were reported. BRL PS showing the luminescence at 702 nm with an excitation wavelength of 400 nm was prepared with two distinct refractive indices by applying alternating current densities. The monolayer PS showed a broad PL spectrum with a full width at half maximum (FWHM) of 125 nm, however, BRL PS exhibited sharp PL peak which reached FWHM of 14 nm. This sharp PL of BRL PS presumably originated from the result of Bragg resonance in PS multilayer. Analysis of cross-sectional FE-SEM images and porosities of BRL PS samples suggests that the sharp PL peak at 700 nm of BRL PS is the second-order luminescence reflectivity peak by Bragg resonance phenomenon. To investigate the Bragg-reflective PL property, the monolayer PS and BRL PS samples were exposed to a vapor flux of acetone. Optical reflectivity and luminescence spectra were measured simultaneously. Analysis on the changes of reflectivity and quenching PL indicated that the larger change in quenching PL of BRL PS compare to that of the monolayer PS, is due to the decrease in enhancement effect of luminescence and also the red shift of Bragg resonance luminescence peak is due to the adsorption by organic vapor in pores.

2.5 References

[1] L. T. Canham. *Appl. Phys. Lett.* 57(10), 1046 **(1990).**

[2] H. Sohn, S. Letant, M. J. Sailor, and W. C. Trogler, *J. Am. Chem. Soc.* 122, 5399 **(2000).**

[3] V. S. Lin, K. Motesharei, K. S. Dancil, M. J. Sailor, and M. R. Ghadiri, *Science* 278, 840 **(1997).**

[4] Y. Koh, S. Jang, J. Kim, S. Kim, Y. C. Ko, S. Cho, and H. Sohn, *Colloid. Surface.* A 313-314, 328 **(2008).**

[5] C. Park, J. Kim, S. Jang, H.-G. Woo, Y. C. Ko, and H. Sohn, *J. Nanosci. Nanotechnol.* 10, 3375 **(2010).**

[6] R. C. Anderson, R. S. Muller, and C. W. Tobias, *Sensor Actuat. A- Phys.* A21-A23, 835 **(1990).**

[7] M. Ben-Chorin, A. Kux, and I. Schechter, *Appl. Phys. Lett.* 64, 481 **(1994).**

[8] J. M. Lauerhaas and M. J. Sailor, *Science* 261, 1567 **(1993).**

[9] C. L. Curtis, V. V. Doan, G. M. Credo, and M. J. Sailor, J. *Electrochem. Soc.* 140, 3492 **(1993).**

[10] S. Kim, B. Cho, and H. Sohn, *Nanoscale Res. Lett.* 7, 527 **(2012).**

[11] S. Jang, J. Kim, Y. Koh, Y. C. Ko, H. -G. Woo, and H. Sohn, *J. Nanosci. Nanotechnol.* 7, 4049 **(2007).**

[12] S. Jang, Y. Koh, J. Kim, J. Park, C. Park, S. J. Kim, S. Cho, Y. C. Ko, H. Sohn, *Mater. Lett.* 62, 552 **(2008).**

[13] S. G. Kim, S. Kim, Y. C. Ko, S. Cho, H. Sohn, *Colloids. Surf A-Physicochem. Eng. Aspects.* 313, 398 **(2008).**

[14] K.-P. S. Dancil, D. P. Greiner, and M. J. Sailor, *J. Am. Chem. Soc.* 121, 7925 **(1999).**

[15] Y. Koh, J. Park, J. Kim, S. Jang, H.-G. Woo, and H. Sohn, *J. Nanosci.*

Nanotechnol. 10, 3590 (2010).

[16] B. Cho, S. Jin, B.-Y. Lee, M. Hwang, H.-C. Kim, and H. Sohn, *Microelectron. Eng.* 89, 92 (2012).

[17] J. H. Song, and M. J. Sailor, *J. Am. Chem. Soc.* 119, 7381(1997).

[18] S. G. Lee, Y. Koh, S. Jang, J. Kim, H.-G. Woo, S. Kim, and H. Sohn, *J. Nanosci. Nanotechnol.* 10, 3266 (2010).

[19] P. Yeh, Optical Waves in Layered Media (USA: Hoboken and NJ Wiley) (1988).

감사의 글

대학원에 입학하여 생활한지 정말 얼마 되지 않은 것 같은데 벌써 졸업할 시기가 다가오고 시간이 정말 빠르게 지나 간 것 같습니다. 대학원 생활을 해온 2년 동안을 돌아보면 정말 많은 생각이 듭니다. 힘들기도 하고 즐겁기도 한 시간이었던 것 같습니다. 여러 방면으로 부족한 저에게 항상 힘이 되어주신 저의 지도교수님이신 손홍래 교수님께 진심으로 감사드리고 항상 교수님께서 주신 가르침을 가지고 사회에 나가서도 열심히 살도록 노력하겠습니다. 또한 고문주 교수님, 이범규 교수님, 류설 교수님, 이종대 교수님, 임종국 교수님 그리고 김호중 교수님까지 항상 관심을 가져 주시고 항상 도움을 주셔서 항상 감사하게 생각 하고 있습니다. 또한 가족보다 더 가족같고 오랜 시간을 함께 지내온 성기오빠, 보민이오빠, 성용이오빠, 종준이오빠, 보미나오빠, 대윤이오빠, 주천이오빠 에게 너무나도 고맙고 항상 여러 방면으로 도움을 주셔서 감사합니다. 무엇보다 대학원 생활을 묵묵히 지켜봐 주시고 믿어 주신 부모님께 정말 감사하고 사랑합니다.

2015년 5월

박 미 애